Proceedings of the Seventeenth International Conference on
Civil, Structural and Environmental Engineering Computing
Edited by: P. Iványi, J. Kruis and B.H.V. Topping
Civil-Comp Conferences, Volume 6, Paper 11.1
Civil-Comp Press, Edinburgh, United Kingdom, 2023
doi: 10.4203/ccc.6.11.1

Rigid Foldable Modular Origami Structure with Negative Poisson's Ratio and Negative Stiffness

C. Chen, Y.T. Bai, S.H. Wang and Z.Y. Wang

School of Civil Engineering, Chongqing University, China

Abstract

Modular origami is a metamaterial that assembles origami or kirigami modules through simple connections such as gluing, which has been little studied in metamaterials. However, it may offer new approaches to the design of mechanical metamaterials due to the unique advantage that material properties and scale do not limit its structure. A novel modular origami structure is developed based on the Miura pattern. It exhibited a significant negative Poisson's ratio and negative stiffness while falling into the rigid folding. Through geometric analysis, we investigate the relationship between the unique kinematics and mechanical properties of this new three-dimensional modular origami structure. In addition, the experiment results showed that the Poisson's ratio of the structure differed remarkably in different directions and is related to the length and angle of each side of the structure. This rigid foldable structure with negative Poisson's ratio and negative stiffness laid a solid foundation for other mechanical metamaterial designs.

Keywords: modular, origami, metamaterial, negative Poisson’s ratio, negative stiffness, foldable.

1 Introduction

Origami, the art of creating three-dimensional structures from two-dimensional sheet mate-rials, originated in ancient China and has been developed significantly in Japan. Origami structures created based on endless crease patterns have been widely used in many fields, such as large-scale foldable aerospace structures[1,2], folded

buildings[3,4], medium-scale self-folding robots[5,6], self-folding biomedical devices[7,8] and nano-folding components[9,10].

As an artificial structure carefully designed by humans, metamaterials have shown colorful and exotic properties, such as lightweight and high strength[11], negative Poisson's ratio[12], and negative stiffness[13]. These properties are not limited by structural scale and material properties, which are hardly visible in traditional natural materials. As a geometric design method, origami structures can use their deployability and reconfigurability to provide unlimited possibilities for designing origami-based metamaterials.

Many essential and innovative results have been achieved in the study of origami structures since 2015. There are 35 publications in Science, Nature, and PNAS, and many papers in the top materials journals, represented by Advanced Materials, and Physics, represented by Physical Review Letters, respectively, as shown in Figure 1. Figure 2 shows the number of journals, conferences, and reviews in the Web of Science (WOS) database searched by the theme "Origami (NOT DNA)" and their citations over the period 1997 to 2022. Over the past two decades, the number of papers published in origami has increased nearly 110-fold, and the number of citations has jumped from zero at the turn of the century to tens of thousands. This fact strongly indicates the rapidly rising and unabated academic interest in origami as a frontier research area.

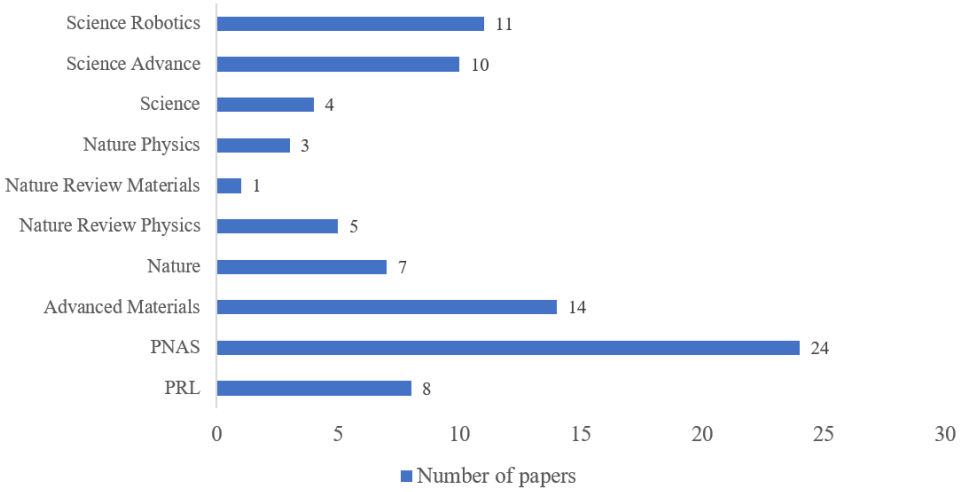

Figure 1: Papers on "Origami (NOT DNA)" published in top journals during 2015-2022.

Rigid origami is an essential branch of origami metamaterials. It means the face remains rigid throughout the folding process along the crease diagram, with only the crease being deformed. That is, rigid origami structures do not require bending or creasing of the face to achieve multiple folds. Standard rigid origami includes Miura-origami (degenerated from 4-degree vertex origami[13]), Waterbomb, and Kresling-origami. The panels theoretically remain rigid during the folding process in rigidly foldable origami, but in reality, they may still deform. This type of deformable origami

involves storing energy in the folds and panels during folding, so they possess a more complex energy landscape and mechanical properties. Deformable rigid origami has been used to absorb impact energy considering the energy absorption of crease folding and panel bending[14-18].

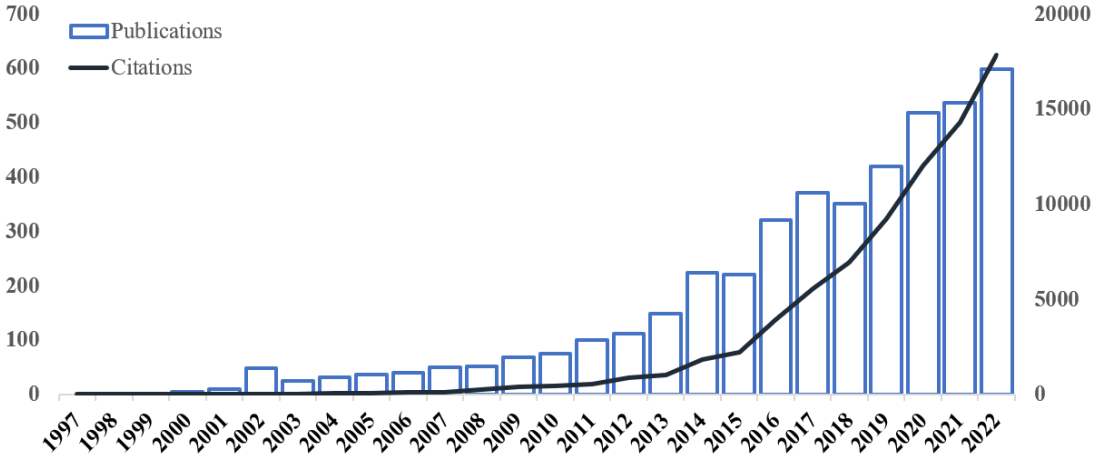

Figure 2: Publications and citations in the WOS database with “Origami(NOT DNA)”.

Therefore, origami-inspired metamaterials should be an essential development direction for various engineering fields in the future. Most origami metamaterials are currently prototyped with paper, and the plasticity and fragility of paper limit their mechanical properties. To design origami metamaterials for real-world applications, materials with different properties, such as metallic materials, should be considered. The folds of origami and the joints of origami are stress concentrations and should be specially designed to resist impacts and improve flexibility. Based on the above background, a new design of origami metamaterial is proposed, and its performance in terms of mechanical behavior is investigated.

2 Design of Modular Origami Structure

Figure 3(a) shows an ori-kirigami unit based on the Miura-Ori pattern, where the solid lines are folds, and the dashed lines are cut marks. The lines AQ, BR, CS, and DT are mountain folds, and GH, OP, and KL are valley folds. A paper unit consists of eight squares and eight small parallelogram blocks, the square side length is a, and the two pairs of parallelogram side lengths are a, b. The ori-kirigami paper unit is folded to obtain a hollow oblique prism structure. The tubular structure is divided into four tiny hollow oblique prisms equally. The small hollow oblique prisms are connected two by two through the joint edge, as shown in Figure 3(b), 3(c) for its rendering, and Figure 3(d) to (f) are the structure drawings obtained by mirroring the said tubular structure 1, 2 and 3 times, respectively. Fig. 3(f) shows the initial state of the studied origami structure, Fig. 3(g) shows the compressed state of the studied origami structure, and Fig. 3(h) shows the fully compressed state of the studied origami structure.

When it is compressed, the individual hollow oblique prisms are separated from the tight-fitting state, the control angle points in the same plane of the four tiny hollow oblique prisms are always in the same plane, and the two adjacent small hollow quadrangles rotate in opposite directions along the co-oblique edges and produce line displacements in the plane.

Due to the repeatability of the structure, the structural units are stacked as a periodic structure for the study. Its initial state and the compression process are shown in Figure 4.

Figure 5 shows a Miura cell whose geometry can be determined by various combinations of parameters. Here, we define a parallelogram with an acute angle γ and bilateral lengths a and b. The angle formed by this parallelogram and the plane XOY is θ, where $\theta \in [0, \pi/2]$, and the other graphical parameters are related as follows:

$$C = a \sin\theta \sin\gamma \tag{1}$$

$$S = b \frac{\cos\theta \tan\gamma}{\sqrt{1+\cos^2\theta \tan^2\gamma}} \tag{2}$$

$$L = a\sqrt{1-\sin^2\theta \sin^2\gamma} \tag{3}$$

$$V = b \frac{1}{\sqrt{1+\cos^2\theta \tan^2\gamma}} \tag{4}$$

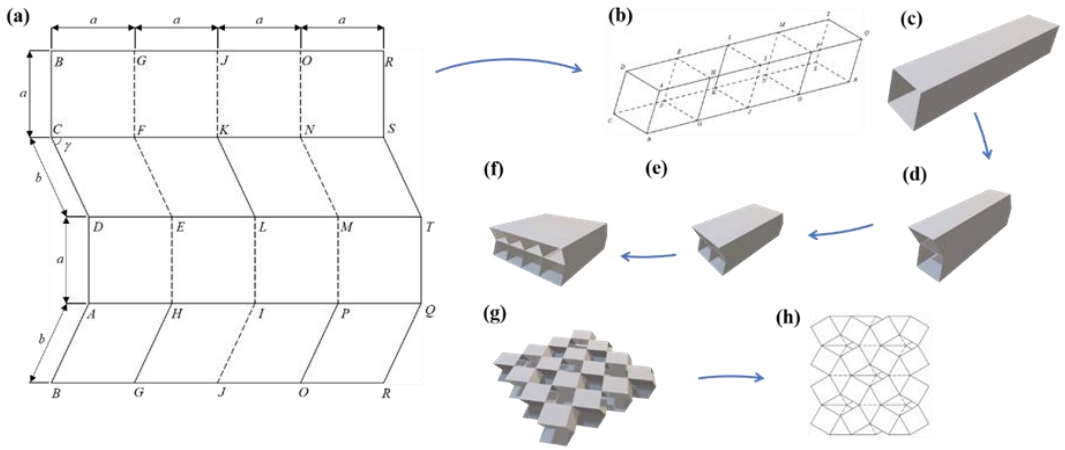

Figure 3: Method of making Origami-Kiri structure.
(a) Ori-kirigami unit crease pattern. (b) (c) Origami-Kiri-based structural unit.
(d) (e) (f) Structures mirrored by (b) 1, 2, and 3 times, respectively.
(g) Structure compression process. (h) The structure is completely flattened.

During the design of metamaterials, the mechanical properties are often characterized in a partially folded state. To illustrate the characterization properties of the structures more efficiently, the following perspectives are introduced:

$$\tan\xi = \cos\theta \tan\gamma \tag{5}$$

$$\sin\Psi = \sin\theta \sin\gamma \tag{6}$$

$$\cos\gamma = \cos\xi \cos\psi \tag{7}$$

$$\sin\varphi = \frac{\sin\xi}{\sin\gamma} \tag{8}$$

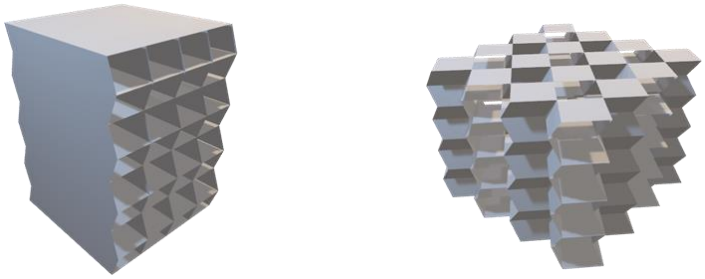

Figure 4: Research object.
(a) Initial state. (b) Compression status.

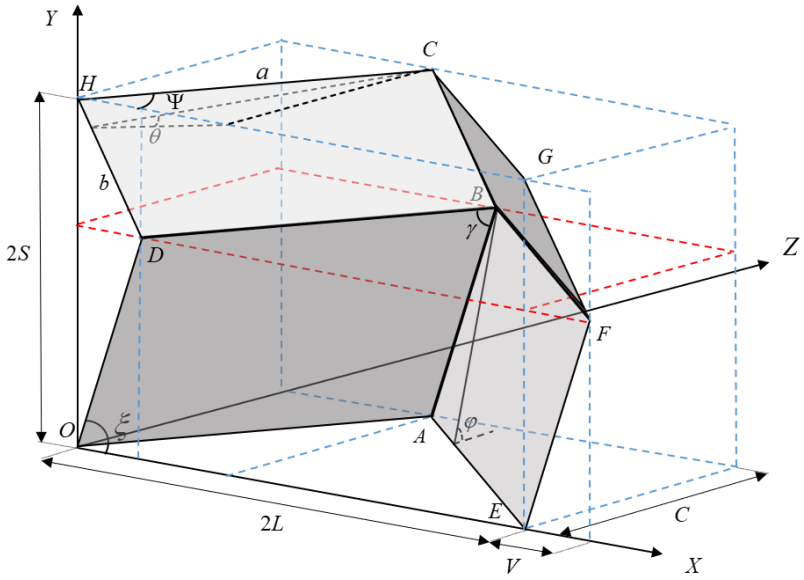

Figure 5: Basic parameter definition of MIURA.

Where $\xi \in [0, \pi/2]$ is the angle between one side of the parallelogram (OD) and the plane XOZ, $\Psi \in [0, \gamma]$ is the angle between the other side of the parallelogram (OA) and the XOY plane, and $\varphi \in [0, \pi/2]$ is the angle between the plane where the parallelogram is located and the plane XOZ.

When the structure is partially separated during deformation, the parameter "T" can express its separation length, as in Figure 6.

$$T = a\cos\Psi \tag{9}$$

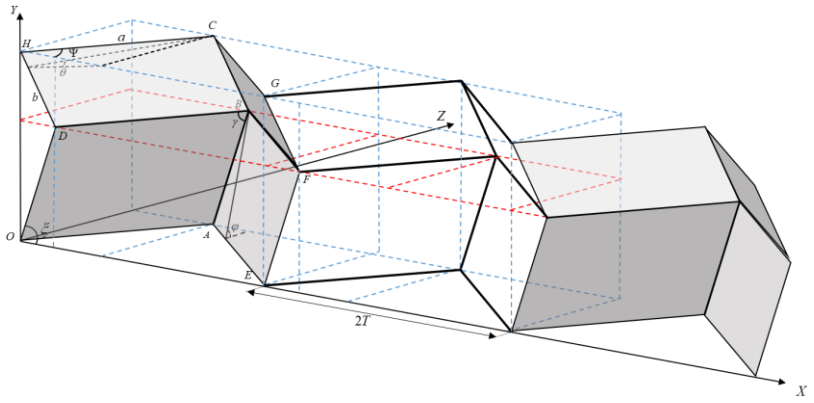

Figure 6: Definition of parameter “T”.

3 Poisson’s Ratio

We use the tiniest cell for Poisson's ratio calculation for computational simplicity and experimental convenience. Here, we define the individual smallest module: the number of each deformable hollow oblique tetragonal prism (consisting of only four planes) is 1, which can be expressed as:

$$N = N_x \times N_y \times N_z = 1\times1\times1 \tag{10}$$

Where N is the total number of modular units, and $N_i\left(i = x, y, z\right)$ is the sum of the numbers in each direction. For the calculation of negative Poisson, we use the specific example of $N = 2\times2\times2 = 8$.

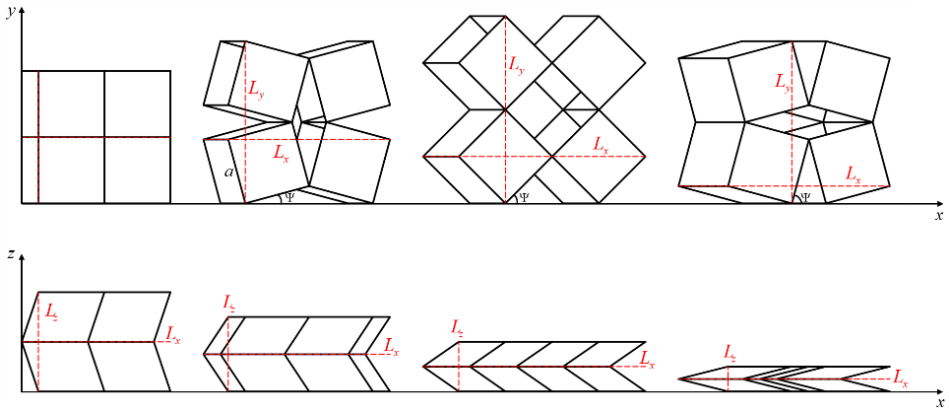

Figure 7: Compression mode of N=8.

Figure 7 shows the compression pattern of a modular origami structure with N = 8. During the compression of the structure, which increases as the structure is compressed, we find that the diagonal of the square above is crossed during the right shift and that bb and cc mutate when a reaches 54°. The specific equation is as follows:

$$L_y = 2a\sin\Psi + 2a\cos\Psi, \quad 0 \le \Psi \le \gamma \tag{11}$$

$$L_x = 2a\sin\Psi + 2a\cos\Psi + b\frac{\cos\gamma}{\cos\Psi}, \quad 0 \le \Psi \le \gamma \tag{12}$$

$$L_z = 4b\sqrt{1-\frac{\cos^2\gamma}{\cos^2\Psi}} \tag{13}$$

$$\nu_{yx} = \frac{dL_y}{L_y} / \frac{dL_x}{L_x} = -\frac{2a\cos 2\Psi - b\tan\Psi\cos\gamma + b\cos\gamma}{2a\cos 2\Psi + b\tan\Psi\cos\gamma + b\tan^2\Psi\cos\gamma}, \quad 0 \le \Psi \le \gamma \tag{14}$$

$$\nu_{yz} = \frac{dL_y}{L_y} / \frac{dL_z}{L_z} = \frac{\cos^2\Psi - \cos\Psi\sin\Psi - \cos^2\gamma + \tan\Psi\cos^2\gamma}{\tan^2\Psi\cos^2\gamma + \tan\Psi\cos^2\gamma}, \quad 0 \le \Psi \le \gamma \tag{15}$$

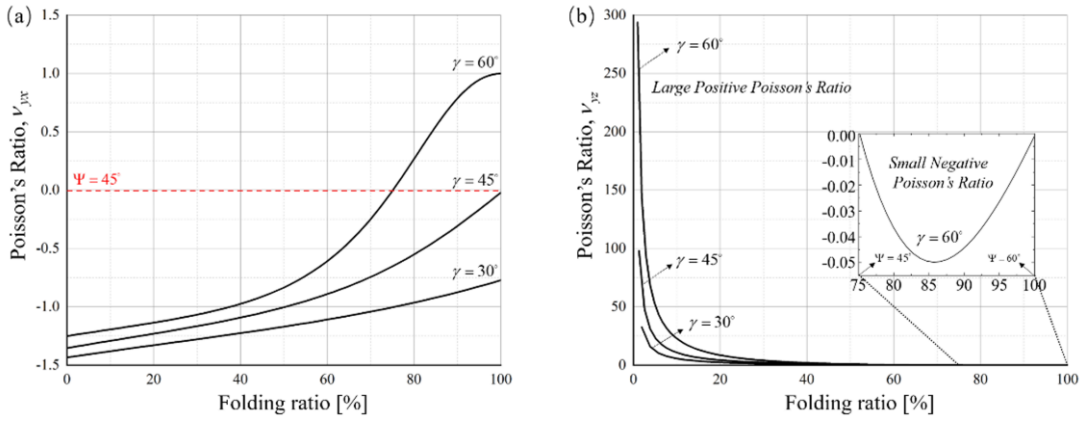

Figure 8: Poisson's Ration of ν_{yx} and ν_{yz}

Figure 8(a) is a transverse Poisson's ratio-folding ratio plot, controlling $a = b = 1$, changing the angle of γ; when $\Psi \le 45^\circ$, the Poisson's ratio is negative. When γ is larger, the initial Poisson's ratio is closer to -1. Controlling γ can make the lateral Poisson's ratio of the structure constant negative or from negative to positive. Figure 8(b) is a longitudinal Poisson's ratio-folding ratio plot, controlling $a = b = 1$, changing the angle of the γ. When $\gamma = 60^\circ$, the structure will have a large Poisson's ratio over a short displacement, up to a maximum of more than 280. At the same time, after the folding rate exceeds 45%, Poisson's ratio tends to 0, and the structure will also have a very weak negative Poisson's ratio, but it can be ignored.

4 Negative Stiffness

Let K_i be the torsional stiffness of the crease, the dihedral angle θ_i as shown in Figure 9, and the total elastic potential energy is the sum of the individual creases, there is:

$$\Pi = \frac{1}{2}K_i\left(\theta_i - \theta_i^0\right)^2 \tag{16}$$

The relationship between displacement and angle can be obtained directly by the modeling software “Rhino-Grasshopper”. The structure has four different dihedral angles. The system's total energy can be obtained using Equation (16).

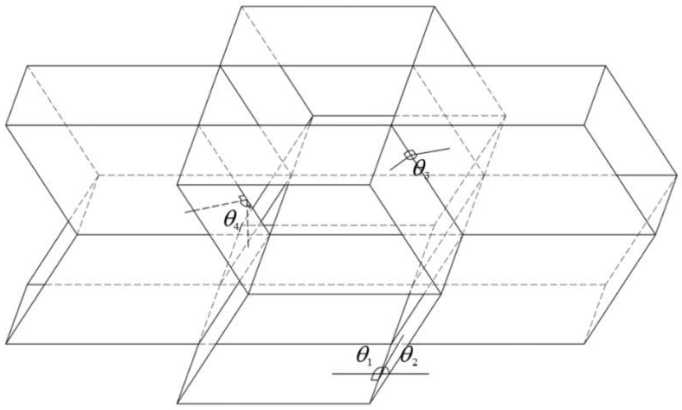

Figure 9: The dihedral angle θ_i.

The energy-displacement curve is obtained by normalizing the displacement, as seen in Figure 10. The force-displacement curve can be obtained by deriving the energy-displacement curve. It can be found that the structure has an extensive range of negative stiffness intervals, which can provide a design method for a high-precision vibration isolation device.

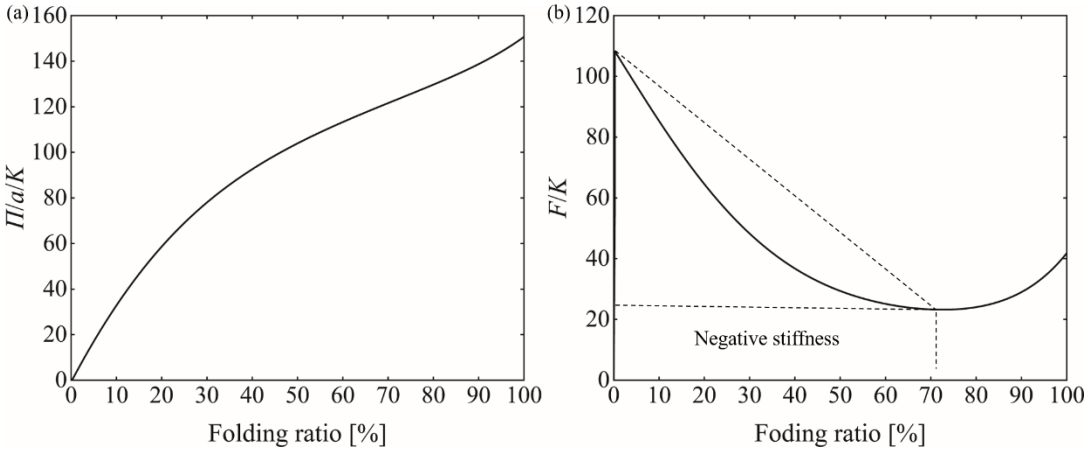

Figure 10:
(a) The relationship between folding ratio and energy;
(b)The relationship between folding ratio and force.

4 Conclusions and Contributions

We designed a rigid foldable origami paper cut structure with a pronounced negative Poisson's ratio, negative stiffness, and other characteristics that ordinary materials do not have. In particular, changing the geometric parameters of the structure can not only make the structure Poisson's ratio achieve positive and negative conversion but

also exaggerate the positive Poisson's ratio. Combined with the instability caused by negative stiffness, the structure can be applied to structural detection units or environments with high requirements for extreme characteristics. The structure does not yet have a unified design approach for topology optimization, which is the next part of the work. Also, whether changing the structural parameters affects Poisson's ratio, stiffness, or even the steady state of the structure is the focus of the work.

References

[1] M. Schenk, A.D. Viquerat, K.A. Seffen, S.D. Guest, "Review of Inflatable Booms for Deployable Space Structures: Packing and Rigidization", Journal of Spacecraft and Rockets 51(3), 762-778, 2014. doi:10.2514/1.A32598

[2] B.N. McPherson, J.L. Kauffman, "Dynamics and Estimation of Origami-Inspired Deployable Space Structures: A Review", AIAA SciTech 2019 Forum, 2019. doi: 10.2514/6.2019-0480

[3] P.M. Reis, J.F. López, J. Marthelot, "Transforming Architectures Inspired by Origami", Proceedings of the National Academy of Sciences, 112(40), 12234–12235, 2015. doi: 10.1073/pnas.1516974112

[4] I. Doroftei, I.A. Doroftei, "Deployable Structures for Architectural Applications: A Short Review", Applied Mechanics and Materials, 658, 233–240, 2014. doi:10.4028/www.scientific.net/AMM.658.233

[5] D. Rus, M.T. Tolley, "Design, Fabrication and Control of Origami Robots". Nature Reviews Materials, Springer US, 3(6), 101–112, 2018. doi:10.1038/s41578-018-0009-8

[6] S. Felton, M. Tolley, E. Demaine, D. Rus, R. Wood, "A Method for Building Self-Folding Machines". Science, 345(6197), 644–646, 2014. doi: 10.1126/science.1252610

[7] C.L. Randall, E. Gultepe, D.H. Gracias, "Self-Folding Devices and Materials for Biomedical Applications", Trends Biotechnical, 30(3), 138-146, 2012. doi: 10.1016/j.tibtech.2011.06.013

[8] K. Kuribayashi, K. Tsuchiya, Z. You, D. Tomus, M. Umemoto, T. Ito, M. Sasaki, "Self-Deployable Origami Stent Grafts as a Biomedical Application of Ni-Rich Tini Shape Memory Alloy Foil", Materials Science and Engineering, 419(1-2), 131–137, 2006. doi:10.1016/j.msea.2005.12.016

[9] L. Xu, T.C. Shyu, N.A. Kotov, "Origami and Kirigami Nanocomposites", ACS Nano, 11(8), 7587–7599, 2017. doi:10.1021/acsnano.7b03287

[10] V.B. Shenoy, D.H. Gracias, "Self-Folding Thin-Film Materials: From Nanopolyhedra to Graphene Origami", MRS Bulletin, 37(9), 847–854, 2012. doi:10.1557/mrs.2012.184

[11] T.A. Schaedler, A.J. Jacobsen, A. Torrents, et al, "Ultralight Metallic Microlattices", Science, 334(6058), 962-965, 2011. doi:10.1126/science.121164

[12] J.N. Grima, K.E. Evans, "Auxetic Behavior from Rotating Squares", Journal of Materials Science Letter, 19, 1563-1565, 2000.

[13] X. Tan, S. Chen, S. Zhu, et al, "Reusable Metamaterial via Inelastic Instability for Energy Absorption", International Journal of Mechanical Sciences, 155,

509-517, 2019. doi:10.1016/j.ijmecsci.2019.02.011
[14] K. Miura, "Method of Packaging and Deployment of Large Membranes in Space", The Institute of Space and Astronautical Science report, 618, 1-9, 1985.
[15] J. Harris, G. Mcshane, "Impact Response of Metallic Stacked Origami Cellular Materials", International Journal of Impact Engineering, 147, 103730, 2021. doi:10.1016/j.ijimpeng.2020.103730
[16] R.J. Ma, Y.T. Wang, M. Li, J. Feng, J.G. Cai, "Study on Coplanar Buffering Performance of Honeycomb Material Based on Miura Origami", Manned Spaceflight, 26(1), 48-55, 2020. doi:10.16329/j.cnki.zrht.2020.01.007
[17] X. Liu, D.H. Li, "Analysis of Axial Impact Performance of Diamond Origami Tubular Structure", Applied Mathematics and Mechanics, 38(2), 163-169, 2017. doi:10.21656/1000-0887.370173
[18] T.H. Zhang, J.Q. Deng, Z.F. Liu, S.Q. Liu, "Compression Deformation and Energy Absorption of Thin-Walled Structures in Curved Origami Pattern", Explosion and Shock, 40(7), 44-52, 2020. doi:10.11883/bzycj-2019-0355